



Features and Prognostic Value of Quantitative Electroencephalogram Changes in Critically Ill and Non-critically Ill Anti-NMDAR Encephalitis Patients: A Pilot Study

Nan Jiang, Hongzhi Guan, Qiang Lu, Haitao Ren and Bin Peng*

Department of Neurology, Peking Union Medical College Hospital, Chinese Academy of Medical Sciences, Beijing, China

OPEN ACCESS

Edited by:

Liping Liu,
Beijing Tiantan Hospital, Capital
Medical University, China

Reviewed by:

Teneille Emma Gofton,
University of Western Ontario, Canada
Benjamin Aaron Emanuel,
University of Southern California,
United States

*Correspondence:

Bin Peng
pengbin3@hotmail.com

Specialty section:

This article was submitted to
Neurocritical and Neurohospitalist
Care,
a section of the journal
Frontiers in Neurology

Received: 08 July 2018

Accepted: 18 September 2018

Published: 05 October 2018

Citation:

Jiang N, Guan H, Lu Q, Ren H and
Peng B (2018) Features and
Prognostic Value of Quantitative
Electroencephalogram Changes in
Critically Ill and Non-critically Ill
Anti-NMDAR Encephalitis Patients: A
Pilot Study. *Front. Neurol.* 9:833.
doi: 10.3389/fneur.2018.00833

Anti-N-methyl-D-aspartate receptor (NMDAR) encephalitis is a common cause of encephalitis in intensive care units. Until now, no reliable method has existed for predicting the outcome of anti-NMDAR encephalitis. In this study, we used quantitative electroencephalography (qEEG) to examine the brain function of anti-NMDAR encephalitis patients and assessed its predictive value. Twenty-six patients diagnosed with anti-NMDAR encephalitis were included and grouped according to whether they were treated in intensive care units (14 critically ill vs. 12 non-critically ill). All patients underwent 2-h 10-channel qEEG recordings at the acute stage. Parameters, including amplitude-integrated electroencephalogram (aEEG), spectral edge frequency 95%, total power, power within different frequency bands (δ , θ , α , and β), and percentages of power in specific frequency bands from frontal and parietal areas were calculated with NicoletOne Software and compared between groups. The short-term outcome was death or moderate/severe disability at 3 months after onset, measured with a modified Rankin Scale, and the long-term outcome was death, disability or relapse at 12 months. No differences in qEEG parameters were observed between the critically ill and non-critically ill patients. However, differential anterior-to-posterior alterations in δ and β absolute band power were observed. Logistic regression analysis revealed that a narrower parietal aEEG bandwidth was associated with favorable long-term outcomes (odds ratio, 37.9; $P = 0.044$), with an optimal cutoff value of 1.7 μV and corresponding sensitivity and specificity of 90.00 and 56.25%, respectively. In a receiver operating characteristic analysis, the area under the curve was 0.7312. In conclusion, the qEEG parameters failed to reflect the clinical severity of anti-NMDAR encephalitis. However, the parietal aEEG bandwidth may separate patients with favorable and poor long-term outcomes in early stages. The underlying mechanisms require further investigation.

Keywords: anti-NMDAR encephalitis, quantitative EEG, amplitude-integrated EEG, prognosis, intensive care unit

INTRODUCTION

Anti-N-methyl-D-aspartate receptor encephalitis is an autoimmune encephalitis involving antibodies directed against the NR1 subunit of the NMDA receptor (NMDAR), and is often associated with ovarian teratomas (1, 2). A considerable proportion of anti-NMDAR encephalitis patients fall into coma or develop status epilepticus and require intensive care. In one retrospective study, anti-NMDAR encephalitis accounted for 1% of all admissions of young adults to intensive care units (ICUs) (3).

Early identification of neurological outcomes is important in terms of therapeutic options. Several prognostic measures have been evaluated in anti-NMDAR encephalitis, including the Glasgow Coma Scale (GCS) score, number of complications, catatonia-predominant type, and electroencephalogram (EEG) (4–6). EEG is a commonly used monitoring tool at the bedside in the ICU, and an EEG “extreme delta brush” (EDB) pattern has been described in anti-NMDAR encephalitis and shown to be a marker of more severe disease and perhaps worse outcome (6). However, the identification of EDB on raw EEG requires experienced raters, which is inconvenient for the continuous monitoring of critically ill patients in the ICU. In addition, the prevalence of EDB is <30% in anti-NMDAR encephalitis patients; therefore, it may not be a sensitive prognostic factor (6–9). Hence, exploration for additional EEG markers to measure severity and predict the outcomes of anti-NMDAR encephalitis is needed, especially for cases where EDB is absent.

A variety of quantitative EEG (qEEG) parameters have been developed in neurocritical care practice, including some applied to the diagnosis of viral encephalitis (10). By applying fast Fourier transformation or other techniques, EEG can be quantified in terms of amplitude, power, frequency, and rhythmicity to generate numerical values, ratios, or percentages (11). Some qEEG parameters may provide quantitative information about short-term and long-term outcomes (11). In this study, we sought to explore features of brain background activity using quantitative analyses of EEG in anti-NMDAR encephalitis patients. The relationships of qEEG characteristics with disease outcomes were also assessed.

METHODS

Participant Enrollment, Data Collection, and Follow-Up

This single-center retrospective observational study was approved by the ethics committee of Peking Union Medical College Hospital. Eligible patients were enrolled from April 2014 to May 2017. Patient consent was not required because de-identified data were used in this study.

All enrolled patients met the diagnostic criteria for anti-NMDAR encephalitis introduced in 2016 (12). Exclusion criteria were as follows: (1) age at onset <12 years; (2) identifiable intracranial infections, other autoimmune encephalitis, or other etiologies causing admission to the ICU; (3) inability to cooperate with qEEG monitoring, due to issues such as agitation; (4) known medical history of a severe neurological deficit [modified Rankin

Scale (mRS), ≥ 2] before onset of anti-NMDAR encephalitis; (5) lack of qEEG recording during the first week of hospitalization in our institute; and (6) missing data or loss to follow-up. According to the severity of disease, patients were further divided into critically ill or non-critically ill subgroups. Patients enrolled in the critically ill subgroup satisfied the following criteria: treated in the ICU for at least 48 h because of (1) GCS ≤ 8 , (2) status epilepticus, or (3) hypoventilation or severe autonomic dysfunction. Patients who did not meet these criteria comprised the non-critically ill subgroup.

We collected the demographic, clinical and laboratory data of patients, including symptoms at the acute stage, serum and CSF studies, and therapeutic regimens. The short-term outcome for this study was death or degrees of disability, which was evaluated with the mRS at 3 months after onset. Patients were considered to have a favorable short-term outcome when their mRS scores were ≤ 2 without increasing compared with baseline, and poor short-term outcome if the mRS scores were ≥ 3 or had increased. Long-term outcomes were obtained from hospital medical records or face-to-face interviews 12 months after onset. Patients with mRS scores ≥ 3 for the whole experimental period or experienced relapse events and received another episode of first-line immunotherapy were defined as experiencing poor long-term outcomes. Patients were considered to have favorable long-term outcomes if their mRS scores were ≤ 2 with no relapse events.

In the final analysis, a total of 26 patients completed 1-year follow-up. Of these, 25 patients were diagnosed with definite anti-NMDAR encephalitis, and 1 patient met the diagnostic criteria for antibody-negative anti-NMDAR encephalitis. We also recruited 10 healthy volunteers with similar ages and collected their qEEG information as a control group.

EEG Recording and Interpretation

qEEG monitoring was performed for at least 2 h for each patient during the first week after admission to our center. Medication administrations during EEG recording were noted and intravenous anti-epileptic agents as well as sedatives were suspended before the start of qEEG monitoring. Silver-chloride disc electrodes were placed according to the International 10–20 System, with a 10-channel layout at the Fp1, F3, C3, P3, O1, and Fp2, F4, C4, P4, O2 sites. The reference electrode was located at Cz, and Fz was used as ground. A 1.0-Hz low- and 35-Hz high-frequency filter was used. Impedances were maintained below 10 k Ω . The qEEG recording was performed using a NicoletOne EEG monitor (VIASYS Healthcare Inc.), and both raw EEG and processed qEEG tracings were sampled simultaneously. The aEEG, spectral edge frequency 95% (SEF-95), total power, power within δ , θ , α , and β frequency bands, as well as relative percentages of power in specific frequency bands were calculated automatically and exported via NicoletOne system.

All qEEG recordings were analyzed off-line. For each patient, we selected one 30-min artifact-free epoch manually from the F3–F4 and P3–P4 montage for further quantitative analysis. We selected F3–F4 as the representative area of the anterior cross-cerebral EEG signal, and P3–P4 as

the representative area of the posterior cross-cerebral EEG signal. Because signals from Fp1-Fp2 and O1-O2 often contain more artifacts or higher impedances, we did not select these recordings for final quantitative analysis.

Statistical Analysis

Descriptive data are presented as mean ± standard deviation (SD) or median with interquartile ranges (IQR). We use Student's *t*-test or the Mann-Whitney *U*-test for group comparisons of continuous variables, and Fisher's exact test for categorical variables, as appropriate. The Kruskal-Wallis test with Bonferroni correction was used for multiple comparisons. Wilcoxon signed rank tests were performed to compare brain activity between anterior and posterior regions. Univariate and multivariate logistic regression with stepwise estimation method was performed to find the independent predictive ability of outcome predictors. Receiver operator characteristic (ROC) curves and areas under the curve (AUC) were constructed to study the ability of aEEG to predict outcomes. For these 2-tailed tests, *p* < 0.05 was considered statistically significant. Statistical analyses were performed using Stata software version 14.1.

RESULTS

Patient Characteristics

Of the 26 patients, 11 (42.3%) were male and 15 (57.7%) were female. The median age was 20 (IQR: 16–27) years. No tumor was found in any of the male patients. Eight (53%) female patients had underlying tumors, which were pathologically confirmed as ovarian teratomas. All patients received intravenous immunoglobulin (2 g/kg divided for 5 days), 25 (96.2%) treated with methylprednisolone (1 g/d for at least 3 days), and 14 (53.8%) patients received second-line immunotherapy. **Table 1** summarizes the comparison of demographic and clinical information between critically ill and non-critically ill patients.

Patient Outcomes

Patient short-term outcomes were as follows: favorable outcome, 7 of 26 (26.9%); and poor outcome, 19 of 26 (73.1%). There was no significant difference between the two subgroups in terms of demographic information, CSF profiles, concomitant tumors, or immunotherapy regimens. All patients in the favorable short-term outcome subgroup had symptoms of impaired memory at admission (7/7 vs. 6/19, *p* = 0.005), and patients with impaired consciousness on admission were more likely to have poor short-term outcomes (1/7 vs. 13/19, *p* = 0.026). Short-term outcomes of the critically ill subgroup were worse than those of the non-critical subgroup (1/7 vs. 13/19, *p* = 0.026).

There were 10 (38.5%) patients experiencing poor long-term outcomes, including 5 with mRS ≥3 and 7 with relapse events within 12 months. One patient died because of complications due to infection. There were no significant differences between the favorable long-term outcome group and poor long-term outcome group in terms of sex, age, clinical

TABLE 1 | Comparison of demographic, clinical, and CSF characteristics between critically ill and non-critically ill patients.

	Critically Ill subgroup	Non-critically Ill subgroup	P-value
DEMOGRAPHIC			
Gender(female)	8/14	7/12	1
Age	20(15,26)	20.5(17,31)	0.502
CLINICAL INFORMATION			
Fever	13/14	4/12	0.003*
Headache	10/14	4/12	0.113
Psychiatric behaviour	12/14	11/12	1
Cognition dysfunction	4/14	6/12	0.422
Memory impairment	4/14	9/12	0.047*
Speech dysfunction	4/14	8/12	0.113
Seizures	13/14	11/12	1
Movement disorder	9/14	6/12	0.692
Central hypoventilation	7/14	0/12	0.006*
Autonomic dysfunction	10/14	5/12	0.233
Decreased consciousness	11/14	3/12	0.016*
Glasgow Coma Scale	5(3,6)	11.5(7,15)	0.005*
Days till diagnosis	20(15,25)	17.5(13.5,34.5)	0.959
Days in hospital	61(54,120)	16.5(13,27.5)	0.0002*
Mechanical ventilation	10/14	0/12	0.0001*
Tumor	7/14	1/12	0.036*
Tumor in female	7/8	1/7	0.01*
Elevated CSF protein	2/14	5/12	0.19
CSF leukocyte			0.728
~5	8/14	6/12	
6~50	5/14	5/12	
51~	1/14	1/12	
Oligoclonal band			0.642
Negative	6/13	3/10	
Suspected	0/13	5/10	
Positive	7/13	2/10	
Antibody titers in CSF			0.324
~1:10	1/14	1/12	
1:32	3/14	5/12	
1:100~	10/14	6/12	
Antibody titers in serum			0.040*
Negative	3/14	7/12	
1:10	2/14	1/12	
1:32~	9/14	4/12	
SECOND-LINE IMMUNOTHERAPY			
MMF	9/14	4/12	0.238
MTX	4/14	0/12	0.100
CTX	1/14	0/12	1
RTX	1/14	1/12	1
No 2nd-line Immunotherapy	4/14	8/12	0.113

**p* < 0.05.

CSF, cerebrospinal fluid; MMF, mycophenolate mofetil; MTX, methotrexate; CTX, cyclophosphamide; RTX, rituximab.

symptoms, severity of onset, duration of hospital stay, profiles in CSF, concomitant tumors, or immunotherapy regimens during hospitalization.

TABLE 2 | Comparisons of qEEG parameters between patients and controls, critically ill patients and non-critically ill patients as well as patients with different outcomes.

	Patients group	Control group	P-value	Critically ill subgroup	Non-critically ill subgroup	P-value	Favorable short-term outcome	Poor short-term outcome	P-value	Favorable long-term outcome	Poor long-term outcome	P-value
Frontal area												
aEEG Upper Margin (μ V)	10.9(9.1,12.4)	10.8(10.1,11.4)	0.860	11.4(8.2,12.8)	10.8(9.7,11.9)	0.918	11(9.1,12.1)	10.7(8.8,12.8)	0.563	10.2(8.3,12.25)	11(10,12.5)	0.257
aEEG Lower Margin(μ V)	8.95(7.4,10.3)	8.9(7.9,9)	0.671	9.3(6.7,11)	8.8(7.9,9.8)	0.959	9(7.4,9.7)	8.9(7.2,11)	0.544	8.4(6.7,10.1)	9.2(8.2,10.3)	0.304
aEEG Bandwidth(μ V)	1.7(1.6,2)	1.9(1.8,2.1)	0.069	1.65(1.5,2)	1.7(1.65,1.95)	0.405	1.8(1.6,2)	1.7(1.6,2)	0.539	1.65(1.55,1.85)	1.8(1.7,2)	0.150
SEF-95(Hz)	1.31(1.24,1.42)	1.39(1.35,1.4)	0.320	1.32(1.29,1.44)	1.31(1.21,1.41)	0.552	1.4(1.31,1.44)	1.31(1.17,1.4)	0.177	1.32(1.23,1.43)	1.3(1.15,1.4)	0.290
Total Power(μ V)	27.86(19.25,61.56)	18.92(16.88,26.01)	0.104	27.04(11.21,64.15)	29.58(20.85,48.95)	0.662	27.86(16.76,35.09)	27.86(19.41,64.59)	0.272	24.82(15.23,50.87)	31.475(25.66,96)	0.257
δ RBP(%)	56.45(40.9,65.39)	54.54(41.08,55.98)	0.397	49.22(39.46,58.37)	61.46(52.31,69.94)	0.143	54.75(39.46,57.53)	58.05(40.9,68.09)	0.563	55.235(40.18,66.43)	57.615(49.86,65.39)	0.732
θ RBP(%)	15.11(11.76,21.13)	16.21(15.32,20.44)	0.572	19.27(11.6,23.9)	14.28(12.54,19.18)	0.700	14.25(11.6,20.61)	17.74(11.76,23.9)	0.803	17.42(12.04,22.515)	14.28(11.21,20.61)	0.544
α RBP(%)	6.18(4.31,10.08)	8.59(7.4,11.56)	0.072	6.59(5.25,11.16)	6.18(4.24,8.56)	0.625	7.86(6.11,10.08)	5.98(4.08,10.42)	0.203	6.03(4.195,8.84)	7.61(5.98,11.16)	0.236
β RBP(%)	10.68(7.44,22.25)	16.38(11.55,18.34)	0.340	12.07(7.54,22.57)	10.60(6.52,16.15)	0.440	14.8(12.01,22.28)	8.34(7.34,22.25)	0.272	10.93(7.49,23.705)	10.175(5.43,20.77)	0.399
δ ABP(μ V)	15.01(8.71,24.34)	8.38(7.03,14.01)	0.148	10.83(6.45,37.88)	16.54(9.88,20.75)	0.520	9.39(6.71,21.6)	16.58(6.37,88)	0.418	12.92(7.9,22.97)	16.59(6.71,37.88)	0.510
θ ABP(μ V)	4.125(2.5,6.93)	3.575(2.39,4.36)	0.427	4.48(1.87,10.84)	4.13(2.58,6.17)	0.939	3.05(2.48,5.57)	4.23(2.5,10.84)	0.355	3.28(2.18,8.16)	4.30(3.06,5.57)	0.580
α ABP(μ V)	1.9150(0.79,4.82)	2.03(1.34,2.64)	0.659	2.17(0.56,5.26)	1.92(0.89,2.51)	0.857	2.26(0.84,2.68)	1.08(0.78,5.26)	0.885	0.890(0.59,4.35)	2.43(1.08,4.82)	0.197
β ABP(μ V)	3.1(1.64,4.25)	3.01(2.01,4.27)	0.646	3.43(1.55,5.18)	2.14(1.70,4.11)	0.738	3.08(1.98,4.25)	3.12(1.55,5.18)	0.862	2.58(1.60,4.18)	3.37(1.98,5.18)	0.693
aEEG Upper Margin (μ V)	10.2(8.8,12.4)	11.4(10.2,13.6)	0.223	9.1(8.12,1)	10.9(9.6,12.6)	0.537	10.8(9.12,8)	10.1(8,12.1)	0.506	9.35(7.8,12.4)	10.95(10.3,12.4)	0.108
aEEG Lower Margin(μ V)	8.45(6.8,10.2)	9.45(8.2,11.4)	0.244	7.25(6.5,10.2)	8.6(7.65,10.35)	0.589	9.1(7.2,10.7)	8.3(6.5,10.2)	0.623	7.45(6.35,10.45)	9.2(8.6,10)	0.170
aEEG Bandwidth(μ V)	1.7(1.5,2)	1.9(1.8,2.1)	0.130	1.65(1.5,2.1)	1.8(1.66,2)	0.393	1.9(1.6,2)	1.7(1.5,2)	0.398	1.6(1.5,1.8)	1.95(1.7,2.1)	0.030
SEF-95(Hz)	1.29(1.19,1.4)	1.38(1.35,1.4)	0.082	1.36(1.24,1.4)	1.23(1.19,1.34)	0.104	1.33(1.22,1.4)	1.29(1.19,1.4)	0.622	1.36(1.21,1.43)	1.24(1.18,1.29)	0.057
Total Power(μ V)	18.88(10.58,33.86)	23.57(14.63,35.69)	0.698	16.51(10.58,43.39)	22.68(10.38,27.9)	0.857	13.84(10.13,28.43)	24.2(10.63,43.39)	0.470	10.689(33.26,47)	27.9(21.16,43.39)	0.022
δ RBP(%)	49.75(41.61,65.05)	39.715(29.78,48.56)	0.024*	51.05(41.61,66.5)	49.75(38.29,61.95)	0.625	49.47(33.66,51.63)	53.04(42.91,67.91)	0.184	49.75(42.66,61.95)	57.11(39.87,67.91)	0.732
θ RBP(%)	16.545(12.94,21.77)	15.72(14.95,17.62)	0.724	16.55(12.94,21.77)	16.89(13.31,21.06)	0.857	15.84(12.07,21.93)	17.04(13.44,21.77)	0.686	16.55(13.19,22.19)	16.89(12.07,20.18)	0.772
α RBP(%)	7.995(5.26,14.93)	13.886(10.14,14.9)	0.066	7.09(4.91,11.94)	12.68(6.78,21.4)	0.143	13.02(10.5,27.48)	7.53(4.43,14.37)	0.073	7.66(4.84,14.65)	9.64(6.65,20.46)	0.414
β RBP(%)	9.765(6.82,15.27)	17.44(14.79,26.7)	0.006*	11.9(8.79,16.62)	8.57(5.66,12.57)	0.165	10.83(6.82,14.89)	9.47(6.11,15.65)	0.644	10.688(8.09,18.48)	8.17(6.11,13.87)	0.114
δ ABP(μ V)	10.095(5.6,13.72)	7.015(3.63,13.56)	0.458	11.5(6.7,20.86)	8.46(5.39,12.73)	0.520	6.61(4.74,11.73)	11.26(5.7,17.38)	0.272	6.48(4.82,12.18)	11.7(9.73,20.86)	0.054
θ ABP(μ V)	2.89(1.47,6.32)	3.675(2.36,5.61)	0.778	2.39(1.35,6.45)	3.48(1.74,6.14)	0.857	2.83(1.35,7.68)	2.95(1.58,6.32)	0.908	1.95(1.34,6.39)	3.83(2.83,6.01)	0.257
α ABP(μ V)	1.755(0.67,4.95)	3.17(1.56,8.07)	0.148	1.160(0.55,4.38)	2.19(1.2,5.63)	0.396	2.38(1.4,6.31)	1.45(0.55,4.38)	0.355	1.17(0.5,4.67)	2.61(1.99,6.31)	0.133
β ABP(μ V)	1.75(1.04,3.05)	4.23(2.63,5.97)	0.008*	2.15(1.04,3.05)	1.33(1.04,2.75)	0.410	2.48(1.43,3.05)	1.58(1.03,3.05)	0.402	1.56(1.01,2.82)	2.24(1.22,3.1)	0.292

* $p < 0.05$.

aEEG, amplitude-integrated electroencephalogram; RBP, relative band power; ABP, absolute band power; SEF-95, spectral edge frequency 95%.

TABLE 3 | The anterior-to-posterior gradient of qEEG parameters in patients and control group.

	Patients group			Critically ill subgroup			Non-critically ill subgroup			Control group			Poor Long-term outcome			Favorable long-term outcome		
	Anterior area	Posterior area	P-value	Anterior area	Posterior area	P-value	Anterior area	Posterior area	P-value	Anterior area	Posterior area	P-value	Anterior area	Posterior area	P-value	Anterior area	Posterior area	P-value
aEEG upper margin	10.85 (9.1,12.4)	10.2 (8.3,12.4)	0.341	11.4 (8.2,12.8)	9.1 (8.12,1)	0.245	10.8 (9.7,11.85)	10.5 (9.6,12.6)	1.000	10.8 (10,11.4)	11.4 (10.2,13.6)	0.103	11 (10,12.5)	10.95 (10.3,12.4)	0.959	10.2 (8.3,12.25)	9.35 (7.8,12.4)	0.224
aEEG lower margin	8.95 (7.4,10.3)	8.45 (6.8,10.2)	0.162	9.3 (6.7,11)	7.25 (6.5,10.2)	0.124	8.8 (7.9,9.8)	8.6 (7.65,10.35)	0.753	8.9 (7.9,9.9)	9.45 (8.2,11.4)	0.047	9.2 (8.2,10.3)	9.2 (8.6,10)	0.759	8.4 (6.7,10.1)	7.45 (6.35,10.45)	0.127
aEEG Bandwidth	1.7 (1.6,2)	1.7 (1.5,1.5)	0.918	1.65 (1.5,2)	1.65 (1.5,2.1)	0.777	1.7 (1.65,1.95)	1.8 (1.65,2)	0.811	1.9 (1.8,2.1)	1.9 (1.8,2.1)	1.000	1.8 (1.7,2)	1.95 (1.7,2.1)	0.603	1.65 (1.55,1.85)	1.6 (1.5,1.8)	0.498
SEF-95	1.31 (1.24,1.42)	1.29 (1.19,1.4)	0.258	1.32 (1.29,1.44)	1.36 (1.24,1.4)	1.000	1.31 (1.205,1.41)	1.23 (1.185,1.34)	0.091	1.39 (1.35,1.4)	1.38 (1.35,1.4)	0.959	1.3 (1.15,1.4)	1.24 (1.18,1.29)	0.240	1.32 (1.3,1.43)	1.36 (1.21,1.43)	0.569
Total power	27.86 (19.25,61.56)	18.88 (10.58,33.86)	0.059	27.04 (11.21,64.15)	16.51 (10.58,43.39)	0.433	29.58 (20.845,48.95)	22.68 (10.38,27.9)	0.050	18.915 (16.88,26.01)	23.57 (14.63,35.69)	0.959	31.475 (25.66,36)	27.9 (21.16,43.39)	0.285	24.82 (15.23,50.87)	10.68 (9.33,26.47)	0.070
δ RBP	56.45 (40.9,65.39)	49.75 (41.61,65.05)	0.638	49.22 (39.46,58.37)	51.045 (41.61,66.5)	0.158	61.46 (52.305,69.94)	49.75 (38.285,61.945)	0.060	54.535 (41.08,55.98)	39.715 (29.78,48.56)	0.005	57.615 (49.86,65.39)	57.11 (39.87,67.91)	0.721	55.235 (40.18,66.43)	49.75 (42.66,61.95)	0.756
θ RBP	15.105 (11.76,21.13)	16.545 (12.94,21.77)	0.409	19.265 (11.6,23.9)	16.545 (12.94,21.77)	0.778	14.28 (12.54,19.175)	16.685 (13.305,21.055)	0.136	16.21 (15.32,20.44)	15.72 (14.95,17.62)	0.333	14.28 (11.21,20.61)	16.69 (12.07,20.18)	0.799	17.42 (12.04,22.515)	16.55 (13.19,22.19)	0.255
α RBP	6.18 (4.31,10.08)	7.995 (5.26,14.83)	0.002	6.59 (5.25,11.16)	7.09 (4.91,11.94)	0.363	6.18 (4.235,8.56)	12.675 (6.78,21.14)	0.002	8.585 (7.4,11.56)	13.885 (10.14,14.9)	0.005	7.61 (5.98,11.16)	9.64 (6.65,20.46)	0.114	6.03 (4.195,8.84)	7.66 (4.84,14.65)	0.005
β RBP	10.675 (7.44,22.25)	9.765 (6.82,15.27)	0.228	12.07 (7.54,22.57)	11.9 (8.79,16.62)	0.470	10.595 (6.52,16.15)	8.575 (5.865,12.57)	0.388	16.38 (11.55,18.34)	17.44 (14.79,26.7)	0.075	10.175 (5.43,20.77)	8.17 (6.11,13.87)	0.241	10.93 (7.49,23.705)	10.68 (8.09,18.48)	0.501
δ ABP	15.01 (8.71,24.34)	10.095 (6.13,17.2)	0.025	10.83 (6.45,37.88)	11.495 (5.7,20.86)	0.363	16.535 (9.875,20.745)	8.46 (5.385,12.725)	0.015	8.36 (7.03,14.01)	7.015 (3.63,13.56)	0.169	16.59 (8.71,37.88)	11.76 (9.73,20.86)	0.169	12.92 (7.9,22.97)	6.48 (4.82,12.18)	0.049
θ ABP	4.125 (2.5,6.93)	2.89 (1.47,6.32)	0.086	4.475 (1.87,10.84)	2.39 (1.35,6.45)	0.198	4.125 (2.58,6.17)	3.48 (1.735,6.135)	0.272	3.575 (2.39,4.36)	3.675 (2.36,5.61)	0.799	4.30 (3.06,5.57)	3.83 (2.83,6.01)	0.799	3.28 (2.18,8.16)	1.95 (1.34,6.39)	0.063
α ABP	1.915 (0.79,4.82)	1.755 (0.67,4.95)	0.304	2.17 (0.56,5.26)	1.155 (0.55,4.38)	0.778	1.915 (0.89,2.505)	2.185 (1.195,5.63)	0.071	2.03 (1.34,2.64)	3.17 (1.56,8.07)	0.047	2.43 (1.08,4.82)	2.61 (1.99,6.31)	0.445	0.89 (0.59,4.35)	1.17 (0.5,4.67)	0.535
β ABP	3.1 (1.64,4.25)	1.75 (1.04,3.05)	0.020	3.43 (1.55,5.18)	2.15 (1.04,3.05)	0.300	2.14 (1.695,4.105)	1.325 (1.04,2.765)	0.019	3.01 (2.01,4.27)	4.23 (2.63,5.97)	0.114	3.37 (1.98,5.18)	2.24 (1.22,3.1)	0.093	2.58 (1.60,4.18)	1.56 (1.01,2.82)	0.088

aEEG, amplitude-integrated electroencephalogram; RBP, relative band power; ABP, absolute band power; SEF-95, spectral edge frequency 95%.

qEEG Findings

The detailed results for qEEG parameters are presented in **Table 2**. Compared with the healthy control group, the δ relative band power in the posterior area was significantly increased ($p = 0.024$) in the anti-NMDAR patient group, while β relative ($p = 0.006$) and β absolute ($p = 0.008$) band power in the posterior area were significantly reduced. The qEEG parameters in anterior area showed no significant differences between the patient group and the control group. There were also no significant differences in qEEG parameters between critically ill and non-critically ill subgroups, or between patients with favorable and poor short-term outcomes. However, in terms of long-term outcomes, the aEEG bandwidth in the parietal area was significantly lower in patients with favorable outcomes than those with poor outcomes (1.6 vs. 1.95 μV , $p = 0.030$). The parietal total power was also significantly lower in the favorable long-term outcome subgroup compared with the poor outcome subgroup (10.68 vs. 27.9 μV^2 , $p = 0.022$).

We also investigated whether the differences in qEEG parameters between anterior and posterior areas were correlated with severities or outcomes (see **Table 3**). In the healthy control group, we found that the aEEG lower margin, δ relative band power, α relative band power, and α absolute band power differed statistically between the anterior and posterior areas. The aEEG lower margin, α relative band power, and α absolute power exhibited a decline from anterior to posterior areas, while δ relative band power showed the opposite trend. However, in the patient group, the differences in aEEG lower margin, δ relative band power, and α absolute power vanished. The gradient of α relative band power still remained, and new gradients of δ absolute band power and β absolute band power appeared in the patient group. The gradients of α relative band power, δ absolute band power and β absolute band power existed in the non-critically ill subgroup, whereas the differences in all parameters disappeared in critically ill subgroup.

Taking the long-term outcome as dependent variable, with univariate logistic regression we screened parietal aEEG upper margin, aEEG bandwidth, SEF-95, and β relative band power as independent variables. Subsequent multivariate logistic regression analysis yielded only one predictor: the parietal aEEG bandwidth (odds ratio, 37.9; 95% confidence interval, 1.11–1295.27; $p = 0.044$). The maximal index of Youden was 1.4625 for a cutoff value of 1.7 μV , with a sensitivity and specificity of 90.00% and 56.25%, respectively. ROC analysis of parietal aEEG bandwidth yielded an area under the curve of 0.7312 (95% CI: 0.572–0.891; **Figure 1**). Furthermore, using another univariate logistic regression analysis, we found that parietal aEEG bandwidth was associated with long-term moderate/severe disability (mRS score ≥ 3) at 12 months (odds ratio, 761.88; 95% confidence interval, 1.53–378836.40; $p = 0.036$), but not associated with relapse events ($p = 0.611$).

DISCUSSION

Anti-NMDAR encephalitis has been recognized as a common cause of encephalitis in ICU. Despite its responsiveness to

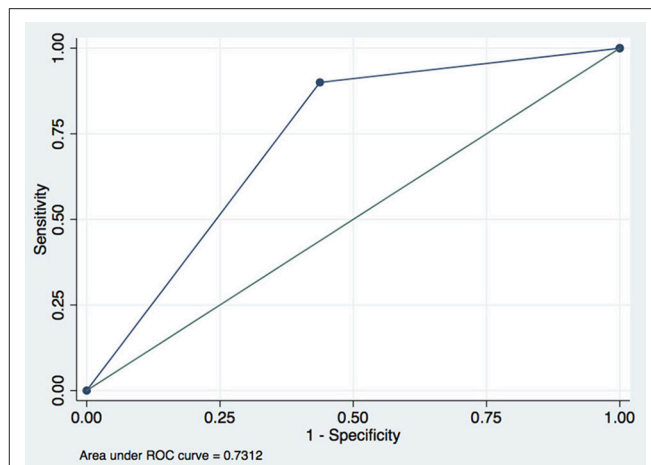
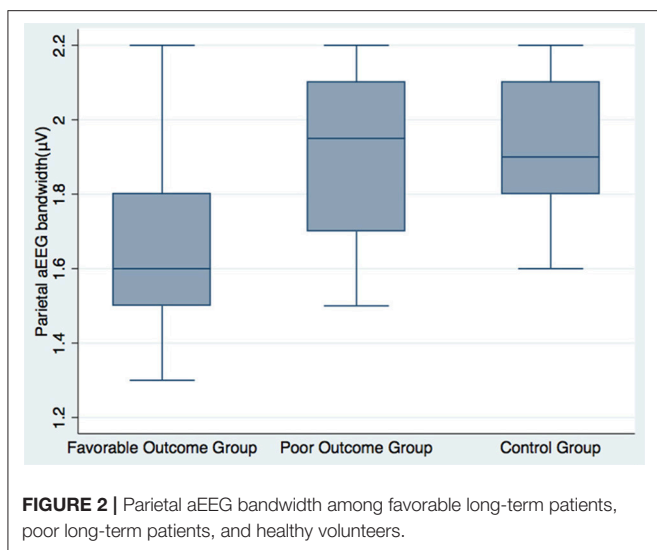


FIGURE 1 | Receiver operating characteristic curve of parietal aEEG bandwidth predicting long-term outcomes of anti-NMDAR encephalitis when cutoff point is 1.7.

immunotherapy and tumor removal, the mortality rate of anti-NMDAR encephalitis in the ICU is 4–25% (4, 13–15). At present, there is no reliable tool for predicting outcomes of anti-NMDAR encephalitis. Most previous electrophysiological studies focused on raw EEG manifestations of anti-NMDAR encephalitis (6, 8, 9). In this study, we investigated the characteristics of qEEG in patients with anti-NMDAR encephalitis. To the best of our knowledge, this is the first study that depicts qEEG findings of patients with anti-NMDAR encephalitis. Our results indicate that most qEEG parameters, including aEEG background, total power, SEF-95, and power of various frequency bands of brain rhythms failed to measure the clinical severity of anti-NMDAR encephalitis. However, the widening of parietal aEEG bandwidth can be used as an objective marker to predict poor long-term outcomes with a good sensitivity.

aEEG is a type of processed EEG that is compressed with respect to amplitude and time, and the upper and lower margins of the aEEG reflect the maximum/minimum peak-to-peak amplitudes of the EEG signals (16). An abnormal aEEG, especially its lower margins, has been shown to be predictive of persistence of severe cerebral injury and poor neurologic outcome (17–19). However, aEEG bandwidth is not a commonly used monitoring marker. The prognostic value of parietal aEEG bandwidth in anti-NMDAR encephalitis is a novel finding and difficult to explain. Previous studies on aEEG have mainly concentrated on disorders that lead to neuron damage, such as stroke, traumatic brain injury, or hypoxic encephalopathy, which can be appraised by aEEG lower margins. However, anti-NMDAR encephalitis selectively reduces NMDAR function and changes the synaptic activities of neuronal networks without any impairment of other synaptic processes (20). Aberrant functioning of a single ion channel may result in various pathophysiological processes (20); therefore, the degree of NMDAR hypofunction may not have a linear



relationship with EEG discontinuity. Thus, the subsequent aEEG changes may be difficult to evaluate using traditional aEEG lower margin. On the contrary, unlike simply measuring the lower margin, aEEG bandwidth may play a diagnostic and predictive role in disorders that are pathogenic to synapses. Specifically, the parietal aEEG bandwidth in healthy controls was wider than in patients with favorable long-term outcomes, and narrower than in those with poor long-term outcomes (Figure 2). This opposite trend suggests that the long-term outcome of anti-NMDAR encephalitis may be determined by underlying, unexplained pathophysiological mechanisms, which might be reflected in electrophysiological parietal aEEG bandwidth. The molecular mechanism underlying this requires further investigation.

Interestingly, compared with healthy controls, the lower margins of the aEEG in both the critically ill and non-critically ill subgroup did not show any significant differences. One possible reason for this phenomenon is the small number of patients. Nevertheless, it may also suggest that brain function in anti-NMDAR encephalitis is relatively intact even in critically ill patients. This characteristic of qEEG is potentially consistent with the pathogenesis of anti-NMDAR encephalitis. NMDAR is an ionotropic glutamate receptor distributed in entire brain tissues. Antibodies directed at the NR1 subunit of the NMDA receptors act by mechanisms including the binding, capping, and cross-linking of NMDA receptors, leading to internalization from the cell membrane surface and a selective decrease in NMDA receptor currents with no effect on synapse number or other synapse proteins (2, 21). The NMDAR hypofunction is non-destructive and reversible, which may explain why the lower margins of aEEG did not decline in the patient group.

Compared with the healthy control group, there were specific anterior-to-posterior graded alterations of qEEG parameters in patients with anti-NMDAR encephalitis. In particular, there were alterations in δ and β absolute band power. δ absolute band power in the posterior area was lower than in the anterior area

in the healthy control group and non-critically ill subgroup, but higher than in anterior area of the critically ill subgroup. However, this trend was reversed in the β absolute band power, which was higher in the posterior area in the healthy control group, and lower in the critically ill and non-critically ill subgroups. Increased power in slower frequency bands (δ and θ) and decreased power in faster frequency bands (α and β) are seen with reductions in brain metabolism (22). No previous studies have reported anterior-to-posterior gradient changes in electrophysiology in anti-NMDAR encephalitis; however, several FDG-PET/CT-based studies have observed specific anterior-to-posterior metabolic gradient changes in the active phase of NMDA encephalitis, and reported these to correlate with disease severity and renormalize with treatment and recovery (23–25). The observed anterior-to-posterior gradient may largely be driven by posterior hypometabolism rather than anterior hypermetabolism (25). Wegener et al. have identified a predominant pattern of frontotemporal hypermetabolism and parietal hypometabolism (26). However, they found that there were no consistent results regarding FD-PET results and impairment as indicated by the mRS (26), which is consistent with our study relative to the prognostic value of the anterior-to-posterior gradient. Another FDG-PET/CT-based study demonstrated marked posterior hypometabolism in patients with anti-NMDAR encephalitis with severe neurologic disability (mRS 4–5), which was more evident than in those less neurologically disabled (mRS 0–3) (25). In our study, the posterior δ absolute band power in non-critically ill subgroup is lower than the anterior area, and this discrepancy disappeared in the critically ill subgroup, which may indicate that more a significant posterior hypometabolism emerged in the critically ill subgroup and supports the research of Probasco et al.

The main limitation of our study is the small number of patients, which limits the power of the findings. In addition, patients requiring qEEG monitoring due to decreased consciousness or suspected seizures, but were not severe enough to require ICU admission, were enrolled as the non-critically ill subgroup. This might have led to a selection bias; however, it also enabled the analysis of the most challenging group of patients with this disease, in whom prognostic biomarkers are most needed. Additional analysis of temporal and occipital areas, as well as prolonged qEEG monitoring, are needed in the future. Furthermore, while critically ill patients are monitored, some were being administered with anti-epileptic drugs, sedatives, or antipsychotics at the same time. In our study, almost all patients in the ICU was administered at least one intravenous sedative, including midazolam, diazepam, or propofol, to control seizures and involuntary movements in the early course of the disease. Before the start of qEEG monitoring, we requested that these sedatives be suspended and restarted after the monitoring is over. However, these medications may still have an impact on EEG signals. In general, sedatives and antiepileptic medications depress the electrocortical activity and render the EEG background more discontinuous and depressed than expected; therefore, a continuous background may become slightly discontinuous (27). If the EEG background is considered normal there is typically no problem with interpretation. In this

study, the aEEG lower margins of all patients were continuous ($> 5 \mu V$); therefore, sedatives and anti-epileptic medications were unlikely to have had a significant impact on our EEG results.

In conclusion, the qEEG pattern in anti-NMDAR encephalitis can offer better understanding of the pathophysiological mechanisms and prognostic possibilities. A wider parietal aEEG bandwidth was associated with worse long-term outcomes, and may serve as a useful biomarker in anti-NMDAR encephalitis. Further, well-designed studies are needed to confirm this novel finding, and elucidate the underlying mechanism.

AUTHOR CONTRIBUTIONS

NJ wrote the initial draft of the paper. HG and HR acquisitioned patients' demographic and clinical data from encephalitis database registration. QL guided for analyzing the EEG signals.

REFERENCES

- Dalmau J, Gleichman AJ, Hughes EG, Rossi JE, Peng X, Lai M, et al. Anti-NMDA-receptor encephalitis: case series and analysis of the effects of antibodies. *Lancet Neurol.* (2008) 7:1091–8. doi: 10.1016/S1474-4422(08)70224-2
- Hughes EG, Peng X, Gleichman AJ, Lai M, Zhou L, Tsou R, et al. Cellular and synaptic mechanisms of anti-NMDA receptor encephalitis. *J Neurosci.* (2010) 30:5866–75. doi: 10.1523/JNEUROSCI.0167-10.2010
- Gable MS, Sheriff H, Dalmau J, Tilley DH, Glaser CA. The frequency of autoimmune N-methyl-D-aspartate receptor encephalitis surpasses that of individual viral etiologies in young individuals enrolled in the California Encephalitis Project. *Clin Infect Dis.* (2012) 54:899–904. doi: 10.1093/cid/cir1038
- Chi X, Wang W, Huang C, Wu M, Zhang L, Li J, et al. Risk factors for mortality in patients with anti-NMDA receptor encephalitis. *Acta Neurol Scand.* (2016) 136:298–304. doi: 10.1111/ane.12723
- DeSena AD, Greenberg BM, Graves D. Three phenotypes of anti-N-methyl-D-aspartate receptor antibody encephalitis in children: prevalence of symptoms and prognosis. *Pediatr Neurol.* (2014) 51:542–9. doi: 10.1016/j.pediatrneurol.2014.04.030
- Schmitt SE, Pargeon K, Frechette ES, Hirsch LJ, Dalmau J, Friedman D, et al. Extreme delta brush: a unique EEG pattern in adults with anti-NMDA receptor encephalitis. *Neurology* (2012) 79:1094–100. doi: 10.1212/WNL.0b013e3182698cd8
- Foff EP, Taplinger D, Suski J, Lopes MB, Quigg M. EEG findings may serve as a potential biomarker for anti-NMDA receptor encephalitis. *Clin EEG Neurosci.* (2016) 48:48–53. doi: 10.1177/1550059416642660
- Zhang Y, Liu G, Jiang MD, Li LP, Su YY, et al. Analysis of electroencephalogram characteristics of anti-NMDA receptor encephalitis patients in China. *Clin Neurophysiol.* (2017) 128:1227–1233. doi: 10.1016/j.clinph.2017.04.015
- Limotai C, Denlerthaikul C, Saraya AW, Jirasakuldej S.. Predictive values and specificity of electroencephalographic findings in autoimmune encephalitis diagnosis. *Epilepsy Behav.* (2018) 84:29–36. doi: 10.1016/j.yebeh.2018.04.007
- Wu Y, Chen M, Cui Y, He X, Niu J, Zhang Y, et al. Viral encephalitis in quantitative EEG. *J Integr Neurosci.* (2018) 17:493–501. doi: 10.3233/jin-180084
- Foreman B, Claassen J. Quantitative EEG for the detection of brain ischemia. *Crit Care* (2012) 16:216. doi: 10.1186/cc11230
- Graus F, Titulaer MJ, Balu R, Benseler S, Bien CG, Cellucci T, et al. A clinical approach to diagnosis of autoimmune encephalitis. *Lancet Neurol.* (2016) 15:391–404. doi: 10.1016/S1474-4422(15)00401-9
- Chen X, Li J-M, Liu F, Wang Q, Zhou D, Lai X. Anti-N-methyl-d-aspartate receptor encephalitis: a common cause of encephalitis in the intensive care unit. *Neurological Sci.* (2016) 37:1993–8. doi: 10.1007/s10072-016-2702-y
- de Montmollin E, Demeret S, Brule N, Conrad M, Dailler F, Lerolle N, et al. Anti-N-methyl-D-aspartate receptor encephalitis in adult patients requiring intensive care. *Am J Respir Crit Care Med.* (2016) 195:491–9. doi: 10.1164/rccm.201603-0507OC
- Harutyunyan G, Hauer L, Dunser MW, et al. Autoimmune encephalitis at the neurological intensive care unit: etiologies, reasons for admission and survival. *Neurocrit Care* (2016) 27:82–9. doi: 10.1007/s12028-016-0370-7
- Zhang D, Ding H. Calculation of compact amplitude-integrated EEG tracing and upper and lower margins using raw EEG data. *Health* (2013) 05:885–891. doi: 10.4236/health.2013.55116
- Hellstrom-Westas L, Rosen I, Svenningsen NW. Predictive value of early continuous amplitude integrated EEG recordings on outcome after severe birth asphyxia in full term infants. *Arch Dis Child Fetal Neonatal Ed.* (1995) 72:F34–8.
- Toet MC, Hellstrom-Westas L, Groenendaal F, Eken P, de Vries LS. Amplitude integrated EEG 3 and 6 hours after birth in full term neonates with hypoxic-ischaemic encephalopathy. *Arch Dis Child Fetal Neonatal Ed.* (1999) 81:F19–23.
- al Naqeeb N, Edwards AD, Cowan FM, Azzopardi D. Assessment of neonatal encephalopathy by amplitude-integrated electroencephalography. *Pediatrics* (1999) 103(6 Pt 1):1263–71.
- Irani SR, Vincent A. NMDA receptor antibody encephalitis. *Curr Neurol Neurosci Rep.* (2011) 11:298–304. doi: 10.1007/s11910-011-0186-y
- Dalmau J, Lancaster E, Martinez-Hernandez E, Rosenfeld MR, Balice-Gordon R. Clinical experience and laboratory investigations in patients with anti-NMDAR encephalitis. *Lancet Neurol.* (2011) 10:63–74. doi: 10.1016/S1474-4422(10)70253-2
- Nagata K, Tagawa K, Hiroi S, Shishido F, Uemura K. Electroencephalographic correlates of blood flow and oxygen metabolism provided by positron emission tomography in patients with cerebral infarction. *Electroencephalogr Clin Neurophysiol.* (1989) 72:16–30.
- Leyboldt F, Buchert R, Kleiter I, Marienhagen J, Gelderblom M, Magnus T, et al. Fluorodeoxyglucose positron emission tomography in anti-N-methyl-D-aspartate receptor encephalitis: distinct pattern of disease. *J Neurol Neurosurg Psychiatry* (2012) 83:681–6. doi: 10.1136/jnnp-2011-301969
- Yuan J, Guan H, Zhou X, Niu N, Li F, Cui L, Cui R. Changing brain metabolism patterns in patients with ANMDARE: serial 18F-FDG PET/CT findings. *Clin Nucl Med.* (2016) 41:366–70. doi: 10.1097/RLU.0000000000001164
- Probasco JC, Solnes L, Nalluri A, Cohen J, Jones KM, Zan E, et al. Decreased occipital lobe metabolism by FDG-PET/CT: an anti-NMDA receptor

BP guided for study designation and made critical revision of draft.

FUNDING

Exploration on the Training Mode of Postgraduate Specialists in Neurology (Item Number 10023201600104).

ACKNOWLEDGMENTS

We gratefully acknowledge the support from Huadong Zhu (Emergency Intensive Care Unit, Peking Union Medical College Hospital, Chinese Academy of Medical Sciences, Beijing, P. R. China) and Bin Du (Medical Intensive Care Unit, Peking Union Medical College Hospital, Chinese Academy of Medical Sciences, Beijing, P. R. China) for their support of this research.

- encephalitis biomarker. *Neurol Neuroimmunol Neuroinflamm.* (2018) 5:e413. doi: 10.1212/NXI.0000000000000413
26. Wegner F, Wilke F, Raab P, Tayeb SB, Boeck AL, Haense C, et al. Anti-leucine rich glioma inactivated 1 protein and anti-N-methyl-D-aspartate receptor encephalitis show distinct patterns of brain glucose metabolism in 18F-fluoro-2-deoxy-d-glucose positron emission tomography. *BMC Neurol.* (2014) 14:136. doi: 10.1186/1471-2377-14-136
27. Hellströmwestas L, Vries LSD, Rosen I. *An Atlas of Amplitude-Integrated EEGs in the Newborn*, 2nd Edn. London: Encyclopedia of Visual Medicine Series (2008).

Conflict of Interest Statement: The authors declare that the research was conducted in the absence of any commercial or financial relationships that could be construed as a potential conflict of interest.

Copyright © 2018 Jiang, Guan, Lu, Ren and Peng. This is an open-access article distributed under the terms of the Creative Commons Attribution License (CC BY). The use, distribution or reproduction in other forums is permitted, provided the original author(s) and the copyright owner(s) are credited and that the original publication in this journal is cited, in accordance with accepted academic practice. No use, distribution or reproduction is permitted which does not comply with these terms.